Resilient Load Frequency Control of Power Systems to Compensate Random Time Delays and Time-Delay Attacks

Xing-Chen Shangguan, *Graduate Student Member, IEEE,* Yong He, *Senior Member, IEEE,* Chuan-Ke Zhang, *Senior Member, IEEE,* Wei Yao, *Senior Member, IEEE,* Yifan Zhao, *Graduate Student Member, IEEE,* Lin Jiang, *Member, IEEE,* and Min Wu, *Fellow, IEEE.*

***Abstract*—Load frequency control (LFC) of modern power systems tends to employ open communication networks to transmit measurement/control signals, which makes the LFC scheme more vulnerable to random time delays and time delay attacks. In this paper, a resilient and active time-delay-compensation-based LFC scheme is proposed to compensate the random time delays and time delay attacks. At first, a state observer is employed to estimate the state of the LFC system. Then a networked predictive control method is used to predict the control signals of the system at the future moments. Next, an evaluation and compensation scheme for random time delays and time delay attacks is constructed in the actuator side of the LFC scheme based on the updating period of the actuator and the timestamp technique. Due to the stochastic characteristics of the random time delays or TDAs, the stability condition of the proposed scheme is developed with the aid of the mean square stability theory. Moreover, a dual-loop open communication is employed in the proposed scheme to improve the reliability and resilience. At last, simulation and experiment tests are undertaken to demonstrate the effectiveness of the proposed scheme.**

***Index Terms*—Power systems, Load frequency control, Random time delays, Time delay attacks, Time delay compensation.**

I. Introduction

A. Research background

Load frequency control (LFC) plays an important role in frequency regulation of power system. The main function of LFC is to remain the balance between load consumption and power generation in the power system, so as to maintain the frequency and tie-line power in the system at a predetermined value [1]. The dedicated communication channel is used to transmit measurements and control signals in the LFC of a traditional power system [2], and may be subjected to small time delays. Such time delays are usually ignored in the control scheme design. However, with the increasing deployment of dispersed renewable energy sources and demand-side responses, an efficient modern power system is suggested to use open communication networks to support these distributed devices [3]. Due to factors such as communication protocol, network loading, and routing over different types of communication lines, random and large time delays are presented in communication links of the open communication networks [4, 5]. Such delays cannot be ignored in the design for an effective LFC scheme and are detrimental to the control performance and the stability of the system [6].

Furthermore, the modern power system is more vulnerable to malicious cyber-attacks, since the shared and open communication network is employed [7–9]. Typical cases include that the management system of supervisory control and data acquisition distribution (SCADA) in Ukraine was attacked by hackers [10] and an Iranian nuclear power station was attacked by the StuxNet virus at Natanz [11]. A time-delay attack (TDA) is a cyber-attack to destabilize the power system by injecting time delays on the sensing loop or control line of the LFC system [12]. Similar to the natural time delay mentioned above, the system control performance will be significantly degraded by time delays from TDAs.

B. Literature review and motivation

Several studies have been completed on the LFC scheme with random time delays or TDAs. The impact of time delays on the traditional and deregulated LFC scheme was discussed and some delay-dependent stability conditions of LFC scheme were derived in [13, 14]. In order to mitigate the adverse impact of time delays, a series of robust PID-type LFC schemes were presented, such as H_∞ thoery [6] and internal model control method [20]. Moreover, a practical LFC is a sampled-data system, as stated in [21, 22]. Considering the sampling characteristic, a robust delay-dependent PI-type LFC scheme was proposed in [23]. Furthermore, to reduce communication burden in power system with a limited communication bandwidth, a series of delay-dependent H_∞ robust LFC schemes were proposed based on event-triggered communication scheme [24–26]. As to TDAs, a state space model of LFC scheme under TDAs was formulated and used

This work was supported in part by the National Natural Science Foundation of China under Grants 62022074 and 61973284, by the Hubei Provincial Natural Science Foundation of China under Grant 2019CFA040, by the 111 project under Grant B17040, and by the "CUG Scholar" Scientific Research Funds at China University of Geosciences (Wuhan) under Grant 2022089. *(Corresponding author: Yong He)*

X.C. Shangguan is with the School of Automation, China University of Geosciences, Wuhan 430074, China, with Shenzhen ET Technology Co., LTD, Shenzhen 518109, China, with Hubei Key Laboratory of Advanced Control and Intelligent Automation for Complex Systems, Wuhan 430074, China, and also with Engineering Research Center of Intelligent Technology for Geo-Exploration, Ministry of Education, Wuhan 430074, China. (email: star@cug.edu.cn)

Y. He, C.K. Zhang and M. Wu are with the School of Automation, China University of Geosciences, Wuhan 430074, China, with Hubei Key Laboratory of Advanced Control and Intelligent Automation for Complex Systems, Wuhan 430074, China, and also with Engineering Research Center of Intelligent Technology for Geo-Exploration, Ministry of Education, Wuhan 430074, China. (email: heyong08@cug.edu.cn; ckzhang@cug.edu.cn; wumin@cug.edu.cn)

W. Yao and Y. Zhao are with the State Key Laboratory of Advanced Electromagnetic Engineering and Technology, School of Electrical and Electronic Engineering, Huazhong University of Science and Technology, Wuhan 430074, China. (email: w.yao@hust.edu.cn;yf_zhao2181@hust.edu.cn)

L. Jiang is with Department of Electrical Engineering and Electronics, University of Liverpool, Liverpool L69 3GJ, United Kingdom.(email: ljiang@liverpool.ac.uk)

to analyse how a TDA to sabotage and destabilize the LFC in [12, 27]. To cope with TDAs, some resilient LFC schemes, which can estimate the TDAs in real time and overcome its effects were proposed in [28, 29]. Nevertheless, only constant or time-varying TDAs were considered in [28, 29] while the random TDAs (RTDAs) are not taken into account. Additionally, countermeasure on RTDAs was proposed in [33] by adopting authenticated timestamp on each data packet to calculate the packet delay and drop the delayed packet. Yet, this countermeasure may generate steady-state control errors and deteriorates the system performance. To address above problems, a perturbation estimation-based robust LFC scheme for power system was introduced, where perturbation term is defined to describe the measurement deviation caused by RTDAs [31].

To sum up, many LFC schemes above are passive control method to cope with the random time delays or TDAs, such as the schemes in [6, 20, 23–26, 33]. However, these schemes are usually robust against a preset time delay. Therefore, the first motivation is to design an active control scheme for LFC system to dynamically compensate to the random time delays or TDAs. Although the active control schemes were proposed for LFC in [28, 31], the schemes are only suitable to deal with the random time delays or TDAs in the sensing loop. If the control lines in LFC are also subjected to random time delays or TDAs, these two schemes may lose their advantages. Then, the second motivation is to design an effective scheme to evaluate the combined time delays in sensing loop, control line and other aspects of the LFC.

On the other hand, the control schemes for networked systems with random time delays or RTDAs have been widely studied. Many passive control schemes have been proposed against random time delays or RTDAs. For example, a robust mixed H_2/H_∞ control was introduced for networked control systems with random time delays in both forward and backward communication links [16], and an observer-based nonlinear H_∞ controller was designed for a class of stochastic non-linear systems subject to the random delays and multiple packet dropouts in [15]. Additionally, many active control scheme have been introduced. For instance, an observer-based incremental predictive control scheme was proposed for the networked multi-agent systems with random delays and packet dropouts in [18], while an output feedback delay compensation control scheme was presented for networked control systems to compensate the random network delay in [19]. However, these schemes cannot address the random time delays and TDAs in control line. To cope with this problem, a networked predictive control scheme was proposed to overcome the effects of network delay and data dropout in [17] and such method has been successfully applied into the wide-area damping control of power system [32]. However, the control performance of the effective scheme in [17, 32] may be degraded when it is used in a practical LFC, due to a large updating period (usually 2-4s) of the power commands in LFC. Therefore, the third research motivation is to design an effective network prediction-based LFC scheme considering the larger updating period characteristics.

C. Contributions

Motivated by the above discussions, a time delay compensation (TDC) scheme based on the network prediction control is proposed for LFC of the power system resilient to *synthetic time delays* (STDs), including natural random time delays and random TDAs. The main contributions as follows.

1) The LFC schemes in [6, 20, 23–26, 33] are all passive and effective for preset time delay. It is difficult to deal with random STDs for these schemes. To address this problem, an active and resilient control scheme based on TDC is proposed for LFC with STDs. The proposed scheme can compensate the random STDs and provide better control performance than the existing LFC schemes.
2) The LFC schemes in [28, 31] are only suitable to deal with the random STDs in the sensing loop, and may be not effective for random STDs in control line or the computational time delay and the waiting time delay. As an improvement, the proposed TDC-based LFC scheme evaluates the STDs based on timestamp technique in the actuator side of the LFC, and can compensate the STDs both in the sensing loop and control line, the computational time delay and the waiting time delay.
3) The networked predictive control scheme in [17, 32] may be not effective in LFC system, since there are a large updating period of 2-4 seconds of the power commands in a practical LFC. To cope with this issue, the updating period of the actuator is set to a large one of $2-4$s in this paper, which is taken into account in modelling and control scheme design of the proposed scheme. Therefore, the proposed scheme caters to the updating characteristic of the power commands in LFC system and ensures the control performance of the proposed scheme under a large updating period.
4) A dual-loop open communication network is suggested to be employed into the proposed TDC-based LFC system. When the time delays are detected to exceed the preset maximum of time delay in the main channel, the main communication channel will be switched to the standby communication channel to mitigate the impact of the severe STDs on the system, so as to improve the reliability and resilience.

The remainder of this paper is organized as follows. Section II presents the sampled-data-based LFC and STD models. Section III introduces the proposed TDC-based LFC scheme. In Section IV, MATLAB simulation tests and experiment tests based on hardware-in-loop are undertaken. Conclusions are presented in Section V.

II. Sampled-data-based LFC and STD models

This section introduces a multi-area LFC model of power system and a synthetic time delay (STD) model for the following design of TDC-based LFC scheme.

A. Multi-area LFC model

A multi-area power system comprises N control areas that are interconnected by tie-lines. The linearized LFC model without the sampling and STDs for area i is presented in Fig. 1 , which includes the governor, the turbine, the rotating mass

and load and the tie-line power. The remote terminal units (RTUs) in a SCADA system are used for acquisition of the measurements (Δf_i and ΔP_{tie-i}). Assume that the generator in every control area is equipped with non-reheat turbine. The equations that govern the dynamics of the i_{th} area are given

$$\begin{cases} \Delta\dot{f}_i(t)=\frac{1}{M_i}(\Delta P_{mi}(t)-\Delta P_{di}(t)-\Delta P_{tie-i}(t)-D_i\Delta f_i(t)) \\ \Delta\dot{P}_{mi}(t)=\frac{1}{T_{chi}}(\Delta P_{vi}(t)-\Delta P_{mi}(t)) \\ \Delta\dot{P}_{vi}(t)=\frac{1}{T_{gi}}\left(\Delta P_{ci}-\frac{1}{R_i}\Delta f_i(t)-\Delta P_{vi}(t)\right) \\ \Delta\dot{P}_{tie-i}(t)=2\pi\sum_{j=1,j\neq i}^{n}T_{ij}\left(\Delta f_i(t)-\Delta f_j(t)\right) \end{cases} \tag{1}$$

where ΔP_{ci}, ΔP_{vi}, ΔP_{mi}, ΔP_{di}, Δf_i and ΔP_{tie-i} denote the control input, the valve position deviation, the generator mechanical output deviation, the load change, the frequency deviation and the tie-line power exchange deviation of the i_{th} area of the power system, respectively; β_i, R_i, M_i, D_i, T_{chi}, and T_{gi} are the frequency bias factor, the speed drop, moments of inertia of the generator, damping coefficient of the generator, time constant of the turbine, and time constant of the governor of the i_{th} area in the power system, respectively; T_{ij} is the tie-line synchronizing coefficient between area i and area j, and $v_i=\sum_{j=1,j\neq i}^{N}T_{ij}\Delta f_j$. ACE_i represents the area control error (ACE) of the i_{th} area and is the linear combination of Δf_i and ΔP_{tie-i}, i.e., $ACE_i=\beta_i\Delta f_i+\Delta P_{tie-i}$.

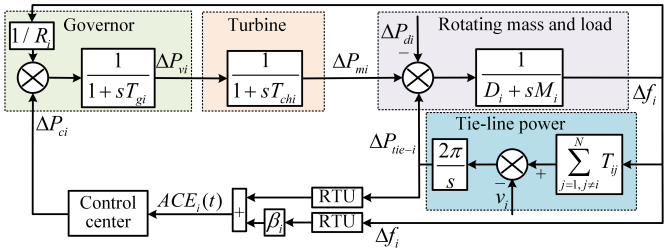

Fig. 1. LFC Structure of area i without sampling and STDs.

To simplify the LFC design, the decentralized control strategy is applied. The exchange of tie-line power in each area is regarded as a disturbance. At this point, the same procedure is used to design the LFC scheme for each control area. The LFC scheme design for a multi-area power system can be treated as a repetitive LFC scheme design of a single area power system. Then, define $x_i=[\Delta f_i,\Delta P_{tie-i},\Delta P_{mi},\Delta P_{vi},\int ACE_i]^T$, $y_i=[ACE_i,\int ACE_i]^T$, and $\omega_i=[\Delta P_{di};v_i]$. The following LFC model of the i_{th} control area can be obtained:

$$\begin{cases} \dot{x}_i(t)=\bar{A}_ix_i(t)+\bar{B}_iu_i(t)+\bar{F}_i\omega_i(t) \\ y_i(t)=\bar{C}_ix_i(t) \end{cases} \tag{2}$$

where

$$\bar{A}_i=\begin{bmatrix} -\frac{D_i}{M_i} & -\frac{1}{M_i} & \frac{1}{M_i} & 0 & 0 \\ 2\pi\sum_{j=1,j\neq i}^{N}T_{ij} & 0 & 0 & 0 & 0 \\ 0 & 0 & -\frac{1}{T_{chi}} & \frac{1}{T_{chi}} & 0 \\ -\frac{1}{R_iT_{gi}} & 0 & 0 & -\frac{1}{T_{gi}} & 0 \\ \beta_i & 1 & 0 & 0 & 0 \end{bmatrix},\ \bar{B}_i=\begin{bmatrix} 0 \\ 0 \\ 0 \\ \frac{1}{T_{gi}} \\ 0 \end{bmatrix}^T,$$

$$\bar{C}_i=\begin{bmatrix} \beta_i & 1 & 0 & 0 & 0 \\ 0 & 0 & 0 & 0 & 1 \end{bmatrix},\ \bar{F}_i=\begin{bmatrix} -\frac{1}{M_i} & 0 & 0 & 0 & 0 \\ 0 & -2\pi & 0 & 0 & 0 \end{bmatrix}^T.$$

The balance point's inner stability of system (2) is equivalent to the origin's stability with $\omega_i(t)=0$. Thus, the state-space model studied in this paper can be rewritten:

$$\begin{cases} \dot{x}_i(t)=\bar{A}_ix_i(t)+\bar{B}_iu_i(t) \\ y_i(t)=\bar{C}_ix_i(t) \end{cases} \tag{3}$$

B. LFC and STD model in sampled-data control mode

In practical, the LFC system is a sampled-data system. The updating period of the control signal is usually 2–4 s. The measurements from the RTUs are not used directly, but are sampled and sent out to the control center at a time interval of T_k. Then, the control signal generated by the control center is updated at a time interval of T_a at the actuator side. Assume that the sensors and the actuators are synchronized and work in a time-triggered mode, while controller works in an event-triggered mode. On the other hand, the signal transmission in the LFC scheme is affected not only by these intervals of T_k and T_a but also by time delays. The detailed process of the signal transmission is shown in Fig. 2.

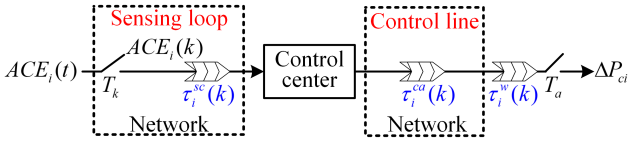

Fig. 2. The process of the signal transmission in LFC with sampling and time delays.

The time delays come from natural random time delays and RTDA. The natural time delays comprise the network-induced delays in sensing loop or control line, the computation delays in control center. As to the RTDA, when time delays are introduced in a control system by a hacker, she or he is performing RTDA. The RTDA can be injected into the measurement signals in the sensing loop and the control signals in the control line. The combined influence of natural time delays and random TDA will be studied in this paper, and their combination is called as *synthetic time delay* (STD). The time delays generated by natural random time delays and RTDAs in the sensing loop and the control line are defined as $\tau_i^{sc}(t)$ and $\tau_i^{ca}(t)$, respectively; the computation time delays are defined as $\tau_i^{com}(t)$; and their combination, STD, is named as $\tau_i^r(t)$. These time delays satisfy

$$0<\tau_i^{sc}(t)+\tau_i^{ca}(t)+\tau_i^{com}(t)=\tau_i^r(t)\leq\tau_{max} \tag{4}$$

where the τ_{max} is the upper bound. With the aid of the sampled-data control, the STD in LFC scheme can be described as a multiple of the sampling period. Assume that the time interval of the actuator is h. Then, STD (4) can be rewritten as follows at the sampling time k.

$$0<\tau_i^{sc}(k)+\tau_i^{ca}(k)+\tau_i^{com}(k)=\tau_i^r(k)\leq mh, m=1,2,\ldots,M. \tag{5}$$

where M is the upper bound, and $mh\leq\tau_{max}\leq Mh$. Note that when a new control signal is sent to the actuator, there is a waiting time delay $0\leq\tau_i^w(k)<h$ before updating the new control signal, as shown in Fig. 2. Therefore, the redefined STD $\tau_i(k)$ for the LFC system can be calculated as follows

$$0<\tau_i(k)=\tau_i^r(k)+\tau_i^w(k)\leq mh, m=1,2,\ldots,M. \tag{6}$$

The value of the waiting time delay varies according to the value of $\tau_i^r(k)$. To clear illustrate the sampling intervals and time delays suffered by the LFC system, the timeline of the signal transmission in LFC system with sampling and STDs is presented in Fig. 3. For example, the measurement $y(0)$ from the sensor will be subjected to $\tau_i^{sc}(0)$ in the sensing loop, then a computational delay of $\tau_i^{com}(0)$ in the control center to obtain the control signal $u(0)$. The control signals will be subjected to a combined time delay of $\tau_i^{ca}(0)$ in the control line. Finally, the control signal $u(0)$ is updated at sampling moment of $2h$ after a waiting time delay of $\tau_i^{w}(0)$ in the actuator. Therefore, the STD in the whole process is $2h$.

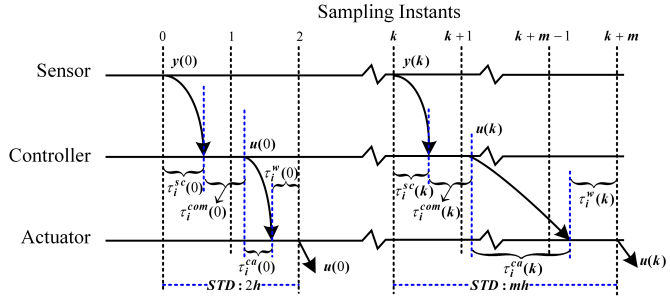

Fig. 3. The timeline of the signal transmission in LFC system with sampling and STDs.

In order to complete the design of the following TDC based LFC scheme, system (3) is discretized and rewritten as follows based on the time interval h of the actuator

$$\begin{cases} x_i(k+1) = A_i x_i(k) + B_i u_i(k) \\ y_i(k) = C_i x_i(k) \end{cases} \tag{7}$$

where $A_i = e^{\bar{A}_i h}$, $B_i = \int_0^h e^{\bar{A}_i h} dt \bar{B}_i$, and $C_i = \bar{C}_i$; $k = 0, 1, 2, 3, \cdots$ are the sampling instants of the sensor and the actuator.

Remark 1: LFC model and the subsequent scheme design of the proposed TDC scheme are established based on the updating period of the actuator. When the updating period is set to $2-4$s, it meets the updating characteristic of power command in LFC and ensures the proposed control scheme operate stably in a large updating period.

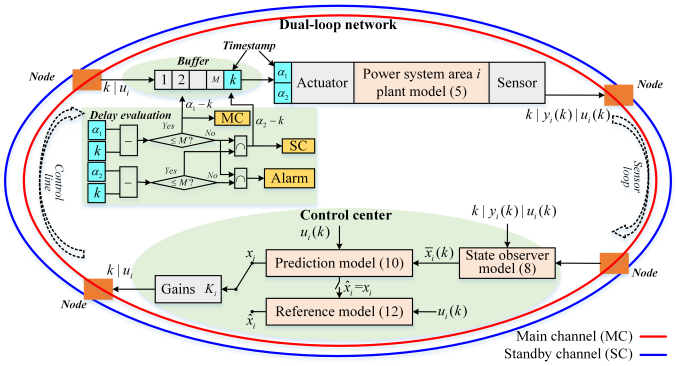

Fig. 4. The schematic of TDC based LFC scheme of area i.

III. Design of the TDC-based LFC scheme

In this section, the design scheme of the TDC-based LFC is proposed. Firstly, the three main aspects of the TDC-based LFC scheme is introduced. Then the stability of the whole control scheme is analyzed. At last, a summarised design procedure for the TDC-based LFC scheme is described.

A. The TDC-based LFC scheme

The TDC-based LFC scheme comprises three parts, the state estimate based on the state observer, the control signal prediction based on system model, and the delay evaluation and compensation based on timestamp. The schematic of the proposed scheme is shown in Fig. 4.

1) State estimate: In the most LFC schemes, frequency Δf_i and tie-line power ΔP_{tie-i} of the ACE are measured and used to design output feedback controller. However, to predict the future control outputs, the full state information of the system is needed in this paper. Therefore, the following Luenberger observer is employed to estimate the system state to avoid to measure the whole states of the LFC system.

$$\bar{x}_i(k+1) = (A_i - L_i C_i)\bar{x}_i(k) + B_i u_i(k) + L_i y_i(k) \tag{8}$$

where L_i is the gain matrix of the state observer. Under sampling instant k, based on the received measurements $y_i(k)$ of the area i and the current control output $u_i(k)$, the observer is designed in control center to estimate the system state $\bar{x}_i(k)$.

Based on the obtained system state, the following state feedback controller is designed to realize the stability of the system without the influence of STDs.

$$u_i(k) = K_i \bar{x}_k \tag{9}$$

where K_i is the state feedback controller gains.

The gains of L_i and K_i are designed in normal operation with no STDs. For convenience, the discrete LQR method is used to obtain the gains via the MATLAB toolbox in this paper.

2) Control signal prediction: In the network prediction control system, the system state estimated $\bar{x}_i(k)$ is regarded as the state $\tilde{x}_i(k)$ of the following prediction model, i.e., $\tilde{x}_i(k) = \bar{x}_i(k)$.

$$\tilde{x}_i(k+1) = A_i \tilde{x}_i(k) + B_i u_i(k) \tag{10}$$

Based on the prediction model, the system state of the future M sampling instants, $\tilde{x}_i(k+1), \ldots, \tilde{x}_i(k+M)$, can be derived by the following equation

$$\tilde{x}_i(k+p) = A_i^p \tilde{x}_i(k) + \sum_{j=0}^{p-1} A_i^j B_i u_i(k), p = 1, \cdots, M. \tag{11}$$

Then, under the action of the state feedback control gains K_i, the control signals at future M sampling instants are obtained by $u_i(k+p) = K_i \tilde{x}_i(k+p)$ with $p = 1, \ldots, M$. The predicted control signals $u_i(k+1)$, …, $u_i(k+M)$ and the current authenticated timestamp kh are packaged together and sent to the buffer of the actuator in the LFC scheme.

In order to prove the stability of the proposed scheme, the following reference model is introduced

$$\hat{x}_i(k+1) = A_i \hat{x}_i(k) + B_i u_i(k) \tag{12}$$

As shown in Fig. 4, the predicted state $\tilde{x}(k)$ is transformed into the reference model, i.e., $\hat{x}(k) = \tilde{x}(k)$, then the control output is updated by $u_i(k) = K_i \tilde{x}(k)$. At this moment, the LFC system is controlled as a closed loop. If a new system state cannot be received by the prediction model, the state of the reference model is used to update the control output. That is $u_i(k) = K_i \hat{x}(k)$. At this point, the LFC system is a open-loop system. Overall, the feedback control law of the whole

TDC-based LFC system is written as follows.

$$u_i(k) = \begin{cases} K_i\hat{x}(k) & open\ loop \\ K_i\tilde{x}(k) & closed\ loop \end{cases} \tag{13}$$

Note that the prediction control signal is calculated based on only the system model. No any objective function is used to optimize the control signals. Specifically, the current state of the system is first estimated by using the state observer, and then the state of the system is predicted at the future time by using equation (11) based on the system model. Then, the control signal of the future time is obtained by the state feedback control law (13).

3) Time delay evaluation and compensation based on timestamp: At first, a dual-loop communication network is suggested to be installed in the proposed scheme. Assume that the main channel and the standby channel are set exactly the same, data are simultaneously transmitted over both channels, and the two channels can switch seamlessly. The time delays in the two channels are monitored and evaluated at the same time.

Then, based on the dual-loop communication network, the time delay evaluation and compensation process is shown in Fig. 4. kh is the timestamp of the signal from the sensor and α_1 and α_2 represent the timestamps when the control signal of the time kh is received at the actuator in the main channel and the standby channel, respectively. The time delays suffered from the main channel and the standby channel can be calculated by $(\alpha_1 - k)h$ and $(\alpha_2 - k)h$, respectively. The control signal $u_i(k + (\alpha_1 - k))$ or $u_i(k + (\alpha_2 - k))$ in the packets will be selected to compensate the time delay when the main channel or the standby channel is used.

To improve the reliability and the resilience of the proposed scheme against severe STDs, the channel switching method is used in the dual-loop communication network. Specifically, when $\alpha_1 - k \leq M$, the main channel is selected to transmit signals; when $\alpha_1 - k > M$ and $\alpha_2 - k \leq M$, the standby channel is selected; when $\alpha_1 - k > M$ and $\alpha_2 - k > M$, the LFC will be interrupted and an alarm will be triggered. Manual repair will be executed until the alarm is cleared, and then LFC will restart. Mh stands for the preset upper bound of the time delay.

Remark 2: Compared with the passive LFC schemes in [6, 20, 23–26, 33], the proposed TDC based LFC scheme is active and can evaluate the STDs and select the control signal obtained by the networked predictive control to compensate the time delay in real-time. Additionally, the evaluation and compensation system for STDs equipped in the actuator side almost takes into account the influence of all random time delays or TDAs in the signal transmission process, which solves the problem that the method proposed in [28, 31] is only suitable for time delays in sensing loop.

Remark 3: The network-induced delay, the computation delay, time delays from TDAs and the waiting delay are not identified and considered in the modelling. Instead, all kinds of time delays are treated as a STD and it is identified based on the timestamp technique at the actuator side. Then, the control signals affected by STD are compensated. It is a convenient way to realize the unified mitigation to the effects of random time delays and TDAs.

Remark4: The usage of the dual-loop communication network will increase the communication cost. However, using only a single channel will increase the risk of LFC system instability due to communication failure or serious cyber-attacks. The instability will cause blackouts of the power system in severe cases. Therefore, it is acceptable to spend certain communication cost of installing one more communication channel so that the dual-loop communication network can improve the reliability and resilience of the LFC system, and enhance the safe and stable operation ability of the LFC system.

B. Stability analysis of the TDC-based LFC system

Based on the section III-A-1), the controller and observer gains of the proposed TDC-based LFC are developed by discrete LQR method. The stability of the proposed TDC-based LFC scheme is guaranteed under these controller and observer gains via the LQR method when the LFC system in the absence of STDs. However, when the proposed TDC-based LFC is subjected to STDs, the LQR has not been used to evaluate the stability. Then, in this section, the stability analysis condition of the proposed TDC-based LFC scheme in the presence of STDs is proposed based on the above controller and observer gains. There are two key steps to obtain the stability analysis condition, as follows.

1) The first step is to obtain the state response of system (7): According to the states of systems (8) , (10) and (12), their error are defined as:

$$\begin{cases} e_3(k) = \hat{x}_i(k) - \tilde{x}_i(k) \\ e_2(k) = \tilde{x}_i(k) - \bar{x}_i(k) \\ e_1(k) = \bar{x}_i(k) - x_i(k) \end{cases} \tag{14}$$

Based on closed-loop control law $u_i(k) = K_i\tilde{x}(k)$, LFC system (7) can be represented by the above error states $e_1(k)$ and $e_2(k)$ as follows:

$$x_i(k+1)=(A_i+B_iK_i)x_i(k)+B_iK_ie_1(k)+B_iK_ie_2(k)$$

Meanwhile, $e_1(k+1) = \bar{x}_i(k+1) - x_i(k+1)$ can be obtained by $e_1(k) = \bar{x}_i(k) - x_i(k)$, and can be rewritten as:

$$\begin{aligned} e_1(k+1) &= L_iC_i(A_i + B_iK_i - I)x_i(k) \\ &\quad + (A_i - L_iC_i - L_iC_iB_iK_i)e_1(k) - L_iC_iB_iK_ie_2(k) \end{aligned}$$

Similarly, $e_2(k+1)$ can be derived by

$$\begin{aligned} e_2(k+1) &= L_iC_i(I - A_i - B_iK_i)x_i(k) \\ &\quad + (L_iC_i - L_iC_iB_iK_i)e_1(k) + (A_i - L_iC_iB_iK_i)e_2(k) \end{aligned}$$

$e_3(k+1)$ can be obtained by

$$e_3(k+1)=A_ie_3(k)$$

That is

$$\begin{cases} x_i(k+1)=(A_i+B_iK_i)x_i(k)+B_iK_ie_1(k)+B_iK_ie_2(k) \\ e_1(k+1)=L_iC_i(A_i + B_iK_i - I)x_i(k) \\ \quad + (A_i - L_iC_i - L_iC_iB_iK_i)e_1(k) - L_iC_iB_iK_ie_2(k) \\ e_2(k+1)=L_iC_i(I - A_i - B_iK_i)x_i(k) \\ \quad + (L_iC_i - L_iC_iB_iK_i)e_1(k) + (A_i - L_iC_iB_iK_i)e_2(k) \\ e_3(k+1)=A_ie_3(k) \end{cases} \tag{15}$$

Defining a new state $\xi_i(k) = [x_i(k), e_1(k), e_2(k), e_3(k)]^T$, then equation (15) can be transformed as

$$\xi_i(k+1) = \Theta\xi_i(k) \tag{16}$$

where

$$\Theta = \begin{bmatrix} A_i + B_iK_i & B_iK_i & B_iK_i & 0 \\ \Theta_1 & \Theta_2 & \Theta_3 & 0 \\ \Theta_4 & \Theta_5 & \Theta_6 & 0 \\ 0 & 0 & 0 & A_i \end{bmatrix}.$$

with $\Theta_1 = L_iC_i(A_i+B_iK_i-I)$, $\Theta_2 = A_i-L_iC_i-L_iC_iB_iK_i$, $\Theta_3 = -L_iC_iB_iK_i$, $\Theta_4 = L_iC_i(I-A_i-B_iK_i)$, $\Theta_5 = L_iC_i-L_iC_iB_iK_i$ and $\Theta_6 = A_i - L_iC_iB_iK_i$.

Defining a new sampling instants as t_k $(k = 1, 2, 3, \cdots)$ when the actuator receives the control signals. The following system state update law can be obtained based on the control law (13)

$$\begin{cases} \tilde{x}_i = \bar{x}_i, t_{k-1} = k - r(t_k) \\ \hat{x}_i = \tilde{x}_i, t_k = k \end{cases} \tag{17}$$

where $r(t_n) = t_n - t_{n-1} \in 1, 2, \cdots, M$ under the impact of $\tau_i(k)$. Then, the following equations can be derived by combining equations (16) and (17).

$$\begin{cases} e_2(t_{k-1}) = 0, & t_{k-1} = k - r(t_k) \\ e_3(t_k) = 0, & t_k = k \end{cases} \tag{18}$$

For the sake of simplicity, system (7) is assumed to start at instant t_0. Based on the above equation, the following equation can be obtained

$$e_2(t_0) = 0 \tag{19}$$

When the initial state $\xi_i(t_0)$ runs at instant t_1^-, the following equation can be obtained

$$e_3(t_1^-) = 0 \tag{20}$$

Then combining (19) and (20), the following equation is derived

$$\xi_i(t_1^-) = \eta_2\Theta^{r(t_0)}\eta_1\xi_i(t_0). \tag{21}$$

Next, the following equations can be developed at instant t_1^+, $\hat{x}_i(t_1^+) - \tilde{x}_i(t_1^+) = \tilde{x}_i(t_1^+) - \bar{x}_i(t_1^+)$

$$\begin{cases} e_2(t_1^+) = 0 \\ e_3(t_1^+) = e_3(t_1^+) + e_2(t_1^+) \end{cases} \tag{22}$$

Based on (21) and (22), the following equation is obtained

$$\xi_i(t_1^+) = \eta_1\eta_3\eta_2\Theta^{r(t_0)}\eta_1\xi_i(t_0) \tag{23}$$

With the aid of the above derivation, the state response system of system (7) can be derived by analogy

$$\xi_i(t_{n+1}) = (\eta_3\eta_2\Theta^{r(t_n)}\eta_1)\cdots(\eta_3\eta_2\Theta^{r(t_0)}\eta_1)\xi_i(t_0) \tag{24}$$

where

$$\eta_1 = \begin{bmatrix} I & 0 & 0 & 0 \\ 0 & I & 0 & 0 \\ 0 & 0 & 0 & 0 \\ 0 & 0 & 0 & I \end{bmatrix}, \eta_2 = \begin{bmatrix} I & 0 & 0 & 0 \\ 0 & I & 0 & 0 \\ 0 & 0 & I & 0 \\ 0 & 0 & 0 & 0 \end{bmatrix},$$

$$\eta_3 = \begin{bmatrix} I & 0 & 0 & 0 \\ 0 & I & 0 & 0 \\ 0 & 0 & 0 & 0 \\ 0 & 0 & I & I \end{bmatrix}.$$

2) The second step is to derive the stability condition: System (24) can be rewritten as the following discrete system:

$$\xi_i(t_{n+1}) = \Psi_{r(t_n)}\xi_i(t_n) \tag{25}$$

where $\Psi_{r(t_n)} = \eta_3\eta_2\Theta^{r(t_n)}\eta_1$.

In LFC scheme, network-induced time delays are presented in communication links of the open communication networks. Note that such delays are random due to factors such as communication protocol, network loading, and routing over different types of communication lines. Additionally, for the time delay attacks, the limitation of attack resources is in conflict with the huge number of sensors, communication facilities and hosts of the power system. A practical solution is to launch random attacks. Consequently, the selected remote signals will only be attacked with a certain probability. Therefore, $r(t_n) \in 1, 2, \cdots, M$ is a set of random variables. Under this case, $r(t_n)$ is assume to have Markov random properties. $1, \cdots, M$ are treated as the Markov random variables, and their state transition probability is written as follows:

$$Pr\{r_{k+1} = j | r_k = i\} = p_{ij}, \forall i, j \in Z^+. \tag{26}$$

The state transition matrix is assumed to be as follows:

$$P_{M\times M}(u, v), u, v \in [1, \cdots, M].$$

Then, state response system (25) of system (7) can be treated as a stochastic system due to the Markov random properties of $r(t_n)$. Therefore, based on the mean square stable theory of a stochastic system, the following theorem can be derived to analyze the stability of the proposed scheme.

Theorem 1: Considering system (25) with zero disturbance. The system is random mean square stable if there are M positive definite symmetric matrices $G_u > 0$ with $u = 1, \cdots, M$, such that, for $u = 1, \cdots, M$, satisfy the following inequalities hold:

$$\Psi_u^T N_u H N_u^T \Psi_u - G_u < 0 \tag{27}$$

where $N_u = [\sqrt{P_{u1}}I, \cdots, \sqrt{P_{uM}}I]$, $H = diag\{G_1, \cdots, G_M\}$.

Proof: The following segmented and random Lyapunov functional is selected:

$$V_n(\xi_i(t_n), r_k) = \xi_i^T(t_n)G(r_k)\xi_i(t_n)$$

where $G(r_k) = G_u > 0$ when $r_k = u$. By defining $\bar{G}_u = \sum_{v=1}^{M} P_{uv}G_v$, then $\bar{G}_u = N_uHN_u^T$ is obtained. Based on the mean square stable theory, the following equation can be derived

$$\begin{aligned} &E\{V_{n+1}((\xi_i(t_{n+1}, r_{k+1}))|\xi_i(t_n), r_k = u) - V_n(\xi_i(t_n), r_k = u)\} \\ &= \xi^T(u)(\Psi_u^T\bar{G}_u\Psi_u - G_u)\xi(u) \\ &= \xi^T(u)(\Psi_u^T N_u H N_u^T \Psi_u - G_u)\xi(u) \end{aligned} \tag{28}$$

If equation (28)< 0, then system (25) is random mean square stable. This completes the proof. ■

Remark 5: By means of the Lyapunov direct method, the stability condition of Theorem 1 is derived via constructing a Lyapunov functional. However, the functional constructed is relatively simple, and the information of the STD is not taken into account. Therefore, the stability condition in Theorem 1 is still conservative.

C. Procedure of the TDC based LFC design

In this subsection, a summarised procedure is introduced to present the design of a resilient TDC-based LFC scheme against STDs. The details are shown in the following algorithm.

Algorithm 1: Design TDC-based LFC scheme.

Step 1 Preset initial system parameters: $\bar{A}_i$, $\bar{B}_i$, $\bar{F}_i$ and $\bar{C}_i$.

Step 2 Set sampling period h and obtain system (7).

Step 3 Set proper matrices Q and R, and apply LQR toolbox to obtain the gain matrices L_i and K_i; select an appropriate M. Equip the designed controllers to each control area. Install a dual-loop communication network into power system.

Step 4 The implementation of the TDC-based LFC scheme.

1) Based on the state observer (8), estimate the system state.
2) Predict the future M system state based on prediction model (10), and calculate the future M control signals based on equations (13) and (17). Then package the M control signals and the current timestamp $t_1 = kh$.
3) The actuator receives the package through the main channel at sampling instant $t_{21} = \alpha_1 h$ and the standby channel at sampling instant $t_{22} = \alpha_2 h$, and stores the package into a buffer. Then the control signal is selected from the buffer.
4) Compare M with $\alpha_1 - k$ and $\alpha_2 - k$, respectively. When $M \geq \alpha_1 - k$, the main channel is selected. If $M < \alpha_1 - k$ and $M \geq \alpha_2 - k$, the communication channel is switched from the main channel to the standby channel. The control signal $u_i(k+(\alpha_1 - k))$ or $u_i(k+(\alpha_2 - k))$ in the packets will be selected to compensate the time delay when the main channel or the standby channel is used. In addition, if $M < \alpha_1 - k$ and $M < \alpha_2 - k$, then an alarm is triggered and the LFC will be interrupted. Execute manual repair until clear the alarm, and then restart LFC.

Remark 6: An appropriate upper bound of time delay M will be determined by combining the following three aspects. First, it is necessary to consider whether the stability condition of the system, Theorem 1, is satisfied. Second, performance evaluation based on simulation test is required, since larger maximum delay will reduce the accuracy of the proposed predictive control method and degrade the control performance. Thirdly, when the time delay exceeds the upper bound of the time delay, the LFC services will be interrupted and an alarm will be triggered. Manual repair will be executed until the alarm is cleared, and then LFC will restart. An excessively small upper bound will cause frequent interruptions of LFC service, resulting in manual maintenance and waste of costs.

IV. Case Studies Based on Simulation and Experiment Test

In this section, the proposed TDC-based LFC scheme for a three-area power system is undertaken in the MATLAB simulation tests and RTLAB experiment tests. The parameters of the three-area LFC system can be found in [25]. To meet the requirements in the practical LFC, the generation rate constraint for every generator and the sampling period of the actuator are set as ± 0.1 pu/min and $h = 4s$, respectively. Moreover, a dual-loop SDH optic fiber open communication networks are applied in the tested systems [34]. The rest of this section will be developed from the following four aspects, control scheme design, MATLAB simulation tests, experimental tests based on hardware-in-loop and robust performance evaluation. The effectiveness and superiority of the proposed TDC-based LFC scheme are demonstrated by comparing with the following three LFC schemes: the state feedback control (SFC) based on state observer without TDC in this paper; the robust exponential decay rate based PI-type (EDRPI) LFC considering sampling and constant time delay proposed in [23]; the robust H_∞ event-triggered PI-type (HETPI) LFC schemes (HETPI-1 in [26] and HETPI-2 in [25]).

A. Control scheme design

To complete the control scheme design, the main task is to obtain the controller parameter and select an appropriate upper bound M of time delay. At first, following the steps of Algorithm 1, the state-feedback controller gains K_i and observer gains L_i can be calculated by using discrete LQR method, and obtained as follows:

Area	gains
1	K_1=−[0.6461 −0.0006 0.0191 0.0234 0.0645]
	L_1=−$\begin{bmatrix} 0.0021 & 0.0283 & -0.0423 & -0.0576 & 0.3565 \\ -0.0005 & 0.0066 & 0.0058 & 0.0076 & 0.3151 \end{bmatrix}^T$
2	K_2=−[0.7745 0.0033 0.0109 0.0257 0.0645]
	L_2=−$\begin{bmatrix} 0.0001 & 0.0294 & 0.0088 & 0.0031 & 0.4003 \\ -0.0004 & 0.0091 & -0.0089 & 0.0088 & 0.3699 \end{bmatrix}^T$
3	K_3=−[0.7763 0.0037 0.0129 0.0225 0.0645]
	L_3=−$\begin{bmatrix} -0.0002 & 0.0300 & 0.0063 & 0.0023 & 0.4014 \\ -0.0004 & -0.0091 & -0.0089 & 0.0088 & 0.3687 \end{bmatrix}^T$

Secondly, it can be found that when M is chosen as $2h-6h$, the TDC-based LFC system is stable based on Theorem 1. The integral time absolute error (ITAE) and integral absolute error (IAE) of the frequency deviation of the three-area LFC scheme based on simulation tests are calculated under different upper bound, and their results are shown in Fig. 5 under five random STDs. It can be seen that when M is $2h$, $3h$ and $4h$, the control performance is basically the same, while the control performance degrades significantly when M changes to $5h$ and $6h$. Considering the costs of manual maintenance and LFC service, $4h$ is an optimal value as the upper bound M of the time delay. Then, the random STDs may exist in the four state of $1h, 2h, 3h$ and $4h$. STDs are assumed to satisfy the following Markov state transition matrix:

$$P_r = \begin{bmatrix} 0.2 & 0.2 & 0.2 & 0.4 \\ 0.2 & 0.4 & 0.1 & 0.3 \\ 0 & 0.2 & 0.3 & 0.5 \\ 0 & 0.5 & 0.2 & 0.3 \end{bmatrix}$$

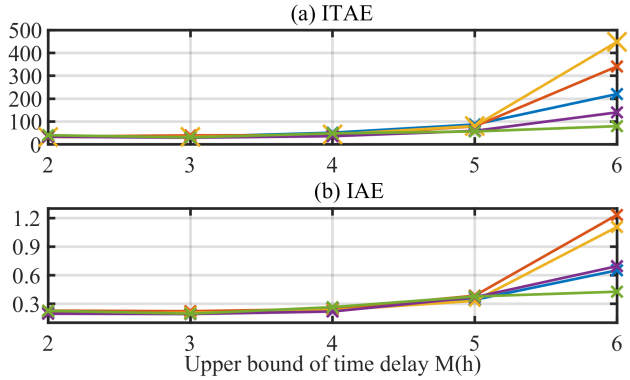

Fig. 5. Performance evaluations for different M under random STDs.

The Markovian time delays $\Gamma_1 - \Gamma_4$ are randomly generated via the MATLAB toolbox and shown in Figs. 6 (a)-(d), respectively. In addition, a slight STD Γ_5 and a serious STD Γ_6 are constructed through the MATLAB random sequence toolbox and displayed in Figs. 6 (e) and (f), respectively. The six STDs will be used in the following tests and exist in the control line. Additionally, every area is assumed to be subjected to a same STD in the three-area LFC system.

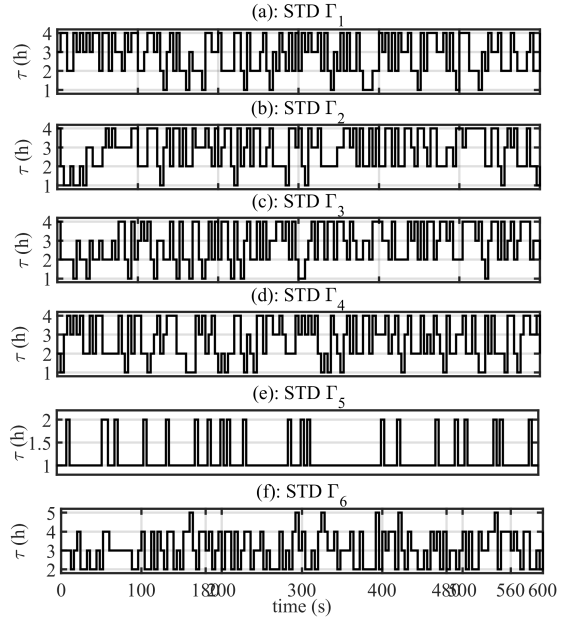

Fig. 6. Random Markovian time delays $\Gamma_1 - \Gamma_4$.

B. MATLAB simulation tests

The three-area LFC system is established in the MATLAB/Simulink platform. In the simulation tests, the system is subject to step changes of load. Area 1, area 2 and area 3 are simultaneously subjected to load changes of 0.01pu, 0.06pu and 0.05pu at $t = 0$s, respectively, and then changed to 0.02pu, 0.01pu and -0.02pu at $t = 300$s, respectively. The changes of load are shown in Fig. 7 (a).

1) Control performance in comparison with the SFC, EDRPI and HETPI: Responses of the frequency deviation, the tie-lie power deviation and the control input of area 1 of power system under STD Γ_1 are displayed in Figs. 7 (b), (c) and (d), respectively. The responses of area 1 under STDs $\Gamma_2 - \Gamma_4$ are similar and omitted here. Additionally, the frequency deviation of area 1 of power system under a slight STD Γ_5 is depicted in Fig. 8. To clear show their differences, the ITAE and IAE of the frequency deviation of three-area LFC scheme under $\Gamma_1 - \Gamma_5$ are calculated and shown in Fig. 9.

As can be seen from Figs. 7 (b)-(d) and 8, the TDC-based LFC scheme proposed can restore the balance between load and generation in a shorter time than SFC LFC scheme, EDRPI LFC scheme in [23] and HETPI LFC scheme in [25, 26]. Especially, the system is divergent under the HETPI LFC scheme in [25]. Moving on to Fig. 9, the performance index, ITAE and IAE of the TDC-based LFC scheme proposed are lower than other control schemes. Firstly, the results illustrate that the proposed TDC-based LFC scheme can operate stably in the sampling period of 4 seconds and provide better control performance than other robust LFC schemes. Secondly, by comparing the proposed TDC-based LFC scheme with the SFC scheme (with out TDC), it can be found from Figs. 7 (b)-(d) and Fig. 9 that the LFC with TDC significantly improves the control performance under STDs $\Gamma_1 - \Gamma_4$, which demonstrates the effectiveness of the proposed TDC scheme. Finally, through a simple repeat test of setting STDs $\Gamma_1 - \Gamma_6$ in the sensing loop, the test results are exactly the same as the

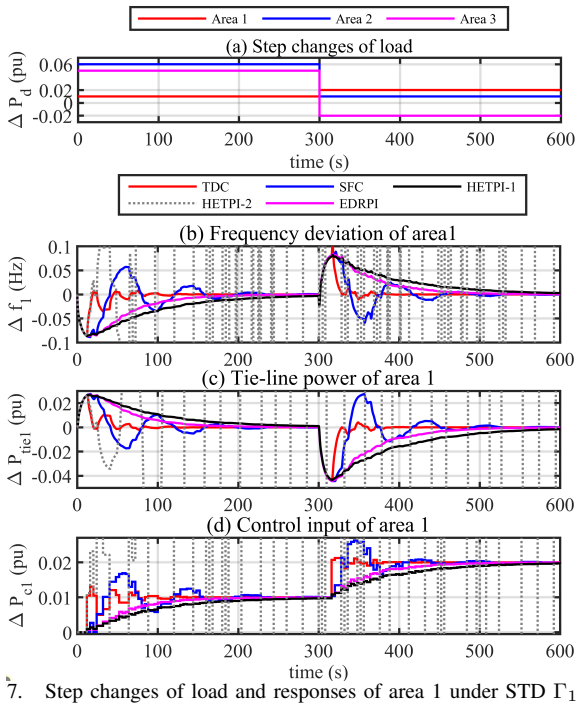

Fig. 7. Step changes of load and responses of area 1 under STD Γ_1.

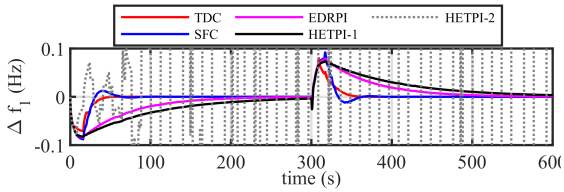

Fig. 8. STD Γ_5 and frequency deviations of area 1 under STD Γ_5.

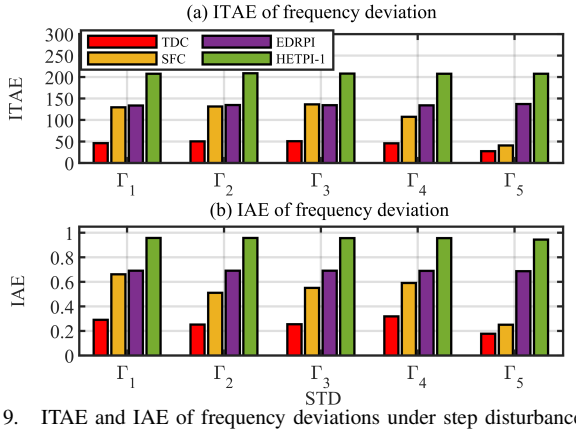

Fig. 9. ITAE and IAE of frequency deviations under step disturbances.

above results of setting these STDs in the control line. This shows that the proposed scheme can deal with the STDs in the control line and illustrates the advantage of designing the TDC-based LFC based on the actuator side in this paper.

2) The advantage of the channel switching: To show the advantage of the channel switching, the responses of the frequency deviations for the three-area LFC without/with channel switching are respectively displayed in Figs. 10 (b) and (c) under the case of severe STD Γ_6. The time of the switching channel is also marked in Fig. 10. Specifically, a severe time delay $5h$ more than $4h$ is detected at the actuator side via the timestamp technique. At this time, the first channel

switching is carried out from the main channel to the standby channel. After 300s, the second channel switching will be performed from the standby channel to the main channel. The third channel switching is undertaken at $t = 560s$ from the main channel to the standby channel when the signals sent at $t = 540s$ experiences a time delay of $5h$. The responses of area 2 and area 3 are similar and omitted here due to space limitation. The ITAE and IAE of the frequency deviation of three-area LFC scheme under Γ_6 with/without channel switching are recorded in Fig. 11. It can be seen from Figs. 10 (b) and (c) and Fig. 11 that the control performance are significantly improved by using the channel switching technique. The adverse impact of a severe STD on the LFC system can be mitigated via channel switching in the dual-loop communication network.

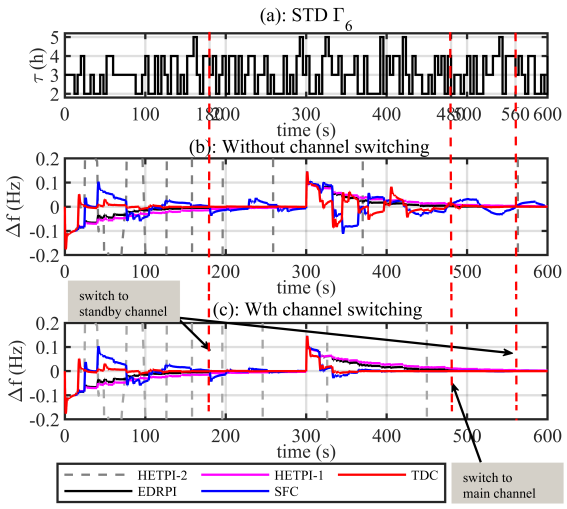

Fig. 10. STD Γ_6 and frequency deviations of area 1 under STD Γ_6.

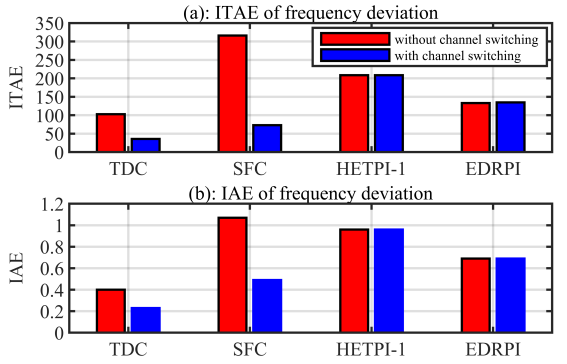

Fig. 11. ITAE and IAE of frequency deviations under step disturbances for STD Γ_6.

C. Experiment tests based on hardware-in-loop

To further verify the effectiveness of the resilient LFC scheme, an experimental test platform of LFC systems has been built based on the real-time simulator OPAL-RT, as shown in Fig. 12. The computer's RTLAB software is used to compile the LFC model and the proposed TDC control model, and load them into the hardware OP4510 and OP5700, respectively. The communication between OP4510 and OP5700 is realized through the signal line. The oscilloscope is applied to display the system responses. In the following tests, the above studied three-area LFC system is compiled and loaded into the hardware. The studied system is tested under step changes of load within 180s. Assume that area 1, area 2 and area 3 are simultaneously subjected to load changes of 0.03pu, 0.02pu and 0.05pu at $t = 0$s, respectively, and then changed to -0.05pu, 0.04pu and -0.03pu at $t = 80$s, respectively. The oscilloscope is applied to record the frequency responses of the tested system.

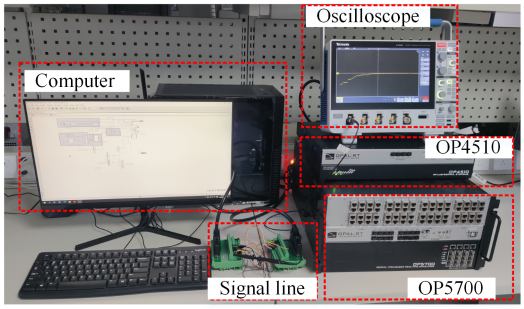

Fig. 12. Experimental test platform of a one-area LFC system.

1) Control performance in comparison with the SFC, EDRPI and HETPI: To validate the effectiveness and superiority of the TDC-based scheme in the experimental tests, the three-area is assumed to be subjected to the STD Γ_3. The frequency deviations of area 1 of the three-area LFC with the TDC, SFC, HETPI-1 and EDRPI schemes under Γ_3 are shown in the Figs. 13-16, respectively. The responses of area 2 and area 3 are similar and omitted here due to space limitation. Moreover, to further illustrate the superiority, the ITAE and IAE of frequency under STDs Γ_3 and Γ_5 are calculated and shown in Fig. 17.

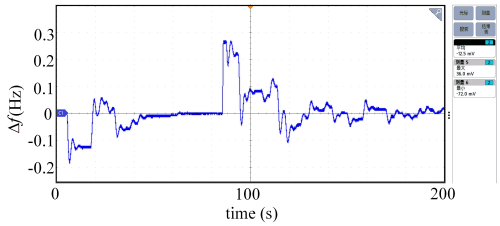

Fig. 13. Frequency deviation of area 1 of the three-area LFC with TDC scheme under Γ_3.

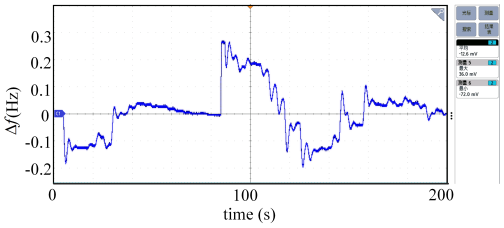

Fig. 14. Frequency deviation of area 1 of the three-area LFC with SFC scheme under Γ_3.

It can be seen from Figs. 13-16 that the TDC-based LFC scheme proposed in this paper can provide faster dynamical performance than SFC scheme, EDRPI scheme in [23] and HETPI-1 scheme in [26]. From the results in Fig. 17, the

values of ITAE and IAE of the proposed TDC scheme are also lower than SFC, EDRPI and HETPI-1 schemes under STDs Γ_3 and Γ_5. Therefore, it can be concluded that the proposed TDC-based LFC scheme is effective under the sampling period of 4 seconds and performs better control performance than other control schemes.

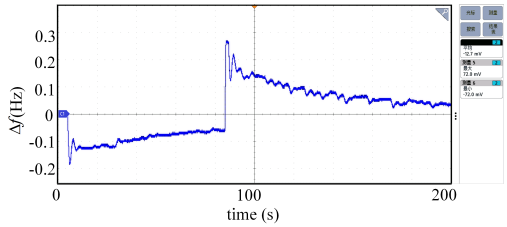

Fig. 15. Frequency deviation of area 1 of the three-area LFC with HETPI-1 scheme under Γ_3.

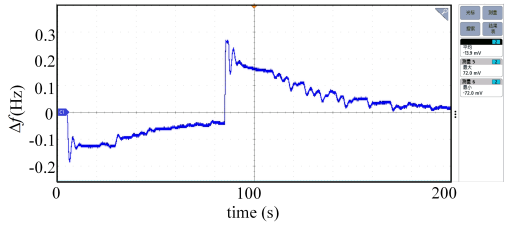

Fig. 16. Frequency deviation of area 1 of the three-area LFC with EDRPI scheme under Γ_3.

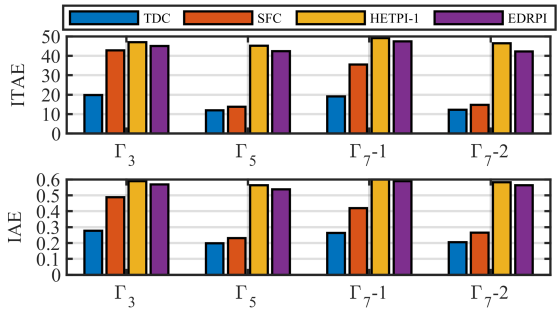

Fig. 17. ITAE and IAE of the three-area LFC in the experimental tests based on hardware-in-loop.

On the other hand, it can be observed from Figs. 13, 14 and 17 that the LFC with TDC significantly improves the control performance of SFC LFC scheme without TDC under STD Γ_3 , which demonstrates the effectiveness of the proposed TDC scheme. Moreover, through a simple repeat test, the test results of setting STD Γ_3 in the sensing loop are totally the same as the above results of setting STD Γ_3 in the control line. This shows that the proposed scheme can deal with the STDs in the control line well and illustrates the superiority of designing the TDC-based LFC based on the actuator side in this paper.

2) The advantage of the channel switching: To show the advantage of the channel switching, the LFC system is tested under random STD Γ_7. As shown in Fig. 18, Γ_7 exceeding the preset upper bound $M = 4h$ occurs at $t = 56$s, then it will be detected by the actuator side after 24s, and the channel switching will be implemented at $t = 80$s. Then, the responses of the frequency deviation of area 1 of the three-area under Γ_7 with/without channel switching are shown in Figs. 19 (a) and (b). The ITAE and IAE of frequency under STD Γ_7 with/without channel switching are all calculated and shown in Fig. 17, where $\Gamma_7 - 1$ represents the results under STD Γ_7 without channel switching and $\Gamma_7 - 2$ represents the results under STD Γ_7 with channel switching.

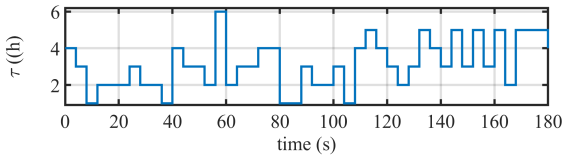

Fig. 18. Random STD Γ_7.

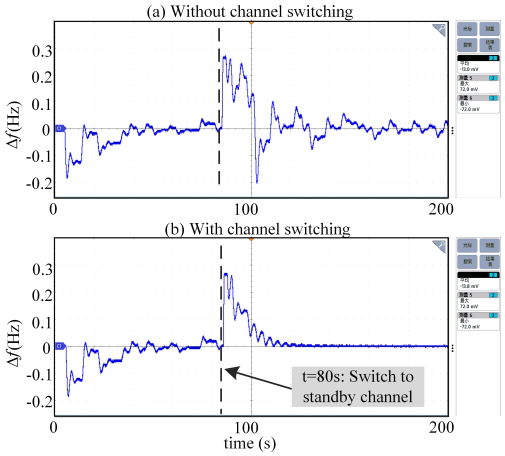

Fig. 19. Frequency deviation of area 1 of the three-area LFC with TDC scheme under Γ_7.

As can be seen from Fig. 19, the control performance is significantly improved by using the channel switching technique at 80s. By referring to the results in Fig. 17, the results of ITAE and IAE under $\Gamma_7 - 2$ with channel switching are also lower than the results under STD $\Gamma_7 - 1$ without channel switching. Therefore, these results demonstrate the advantage of the channel switching method proposed in this paper.

D. Robustness performance evaluation

In this subsection, the proposed TDC-based LFC scheme of the three-area power system is undertaken with parameter variations (PVs) and random packet losses (RPLs) to show the robustness. In the following tests, assume that the system parameters M, D, T_{ch} and T_g are subjected to PVs of $[-25\%, +25\%]$. Additionally, the system is assumed to suffer from three different types of random packet losses (RPLs), as shown in Fig. 20.

In the MATLAB simulation tests, the proposed scheme is tested under STD Γ_1. The results of ITAE and IAE of frequency deviations are recorded in Fig. 21. Additionally, in the experimental tests based on hardware-in-loop, the proposed scheme is tested under STD Γ_3, and their ITAE and IAE of frequency deviations are recorded in Fig. 22.

It can be seen from Fig. 21 that the performance index ITAE and IAE of the proposed TDC-based LFC scheme increase with the introduction of PVs and RPLs. That is, the control

performance of the proposed scheme will degrade under the effect of PVs and RPLs. However, the ITAE and IAE of the proposed scheme are less than 90 and 0.5 under the given PVs and RPLs, respectively. Moving on to the results recorded in Fig. 9, the performance index ITAE and IAE of SFC, EDRPI and HETPI schemes are all more than 100 and 0.6, respectively. Therefore, the control performance of the proposed TDC-based scheme with PVs and RPLs is still better than that of other control schemes without PVs and RPLs. Moreover, it can be observed from Fig. 22 that the control performance is slightly reduced when the system is subjected to RPLs, while the control performance is basically same when the system subjected to PVs. To sum up, these test results show the good robustness of the proposed scheme against certain PVs and RPLs by simulation and experiment tests.

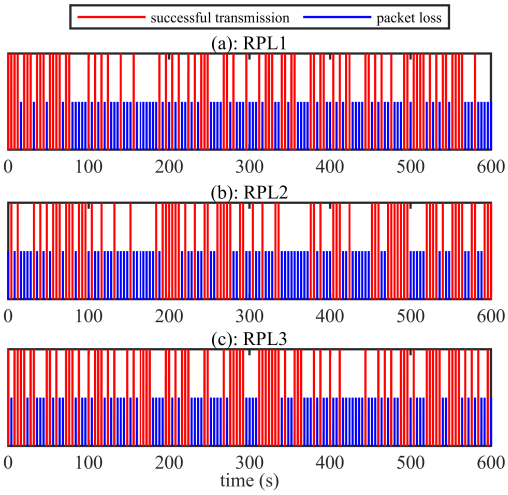

Fig. 20. Random packet losses.

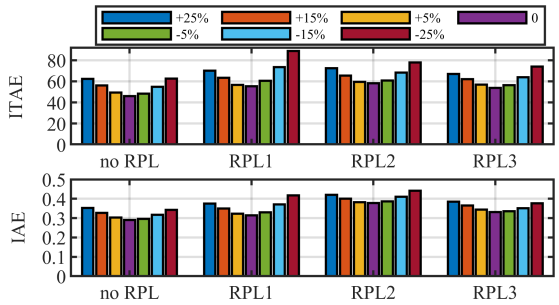

Fig. 21. ITAE and IAE of frequency deviation of the three-area LFC with PVs and RPLs under step changes of load in the MATLAB simulation tests.

Remark 7: The LFC system may be subjected to false data injection (FDI) attack, denial-of-service (DoS) attack and replay attack in addition to the time delay attack. Since the state estimation may be manipulated in FDI attack and the DoS attack will result in the data packet losses, the scheme proposed in this paper cannot be extended to compensate for FID and DoS attacks. In the replay attack, some packets received by the actuator are copied and re-dispatched by the attacker. If the timestamp is added to the packet, the timestamp is not modified when copying the packet. Under this case, when the re-distributed packets are sent to the actuator, the time delay of the packet can be evaluated by comparing the timestamp of the actuator and the timestamp of the packet, then the method proposed can be extended to compensate it.

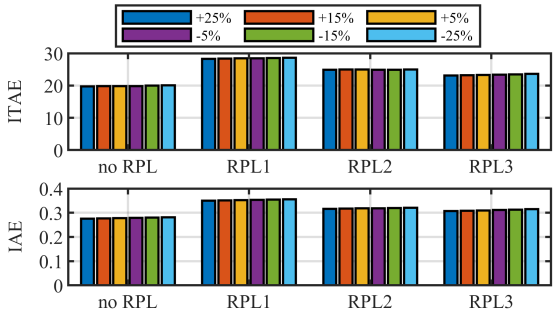

Fig. 22. ITAE and IAE of frequency deviation of the three-area LFC with PVs and RPLs in the experimental tests.

*Remark 8:*The signal transmission in LFC system may be subjected to packet loss, packet disorder and clock jitter. The packet disorder can be dealt with based on the proposed control scheme. It is assumed that the LFC system uses a single packet to transmit signals, rather than using a multi-packet transmission. Under this case, regardless of whether the received data packet is sent from the control center first or later, the predicted control signal can be selected to compensate the time delay based on the time when the packet is received in the actuator side. The clock jitter is usually a deviation with a shorter time. In this paper, the STDs may exist in a form of $h, 2h, 3h, \cdots$ with $h \in (2, 4)$s. When the timestamps of the packet are used to evaluate the time delay, the clock jitter is relatively small with respect to the time delay. Therefore, the influence of clock jitter on the control scheme is ignored. Although the packet loss is not considered, the proposed control scheme has still good robustness to packet loss.

V. Conclusion

A resilient and active TDC-based LFC has been proposed for multi-area power systems to alleviate the impact of STDs. The mean square stability of the proposed scheme has been analyzed when the system is subject to a random Markovian STD. In addition, a dual-loop communication network is installed in the proposed scheme to improve the reliability and resilience. The simulation and experimental tests based on the three-area LFC scheme are undertaken. In the test results, the STDs suffered by the LFC are effectively evaluated by the proposed TDC scheme in real-time and the control performance is significantly improved by compensating STDs based on the predictive control signals. The channel switching method based on the dual-loop open communication network is proved to alleviate the adverse effect of severe STDs on system performance. Additionally, the better robustness of the proposed scheme against parameter uncertainties and random packet losses have been verified. The future research direction is prospected to use robust state observer or optimal predictive control scheme to improve the performance of the proposed control scheme.

REFERENCES

[1] H. Bevrani. *Robust Power System Frequency Control*. New York: Springer, 2014.

[2] H. Shayeghi, H. A. Shayanfar, A. Jalili, "Load frequency control strategies: A state-of-the-art survey for the researcher," *Energy Convers. Manage.*, vol. 50, no. 2, pp. 344-353, Feb. 2009.

[3] V. P. Singh, N. Kishor, P. Samuel. "Distributed multi-agent system-based load frequency control for multi-area power system in smart grid," *IEEE Trans. Ind. Electron.*, vol. 64, no. 6, pp. 5151–5160, June 2017.

[4] W. Yao, L. Jiang, Q. H. Wu, et al. "Delay-dependent stability analysis of the power system with a wide-area damping controller embedded," *IEEE Trans. Power Syst.*, vol. 26, no. 1, pp. 233–240, Feb. 2011.

[5] H. Luo, I. A. Hiskens, Z. Hu. "Stability analysis of load frequency control systems with sampling and transmission delay," *IEEE Trans. Power Syst.*, vol. 35, no. 5, pp. 3603–3615, Sept. 2020.

[6] C. K. Zhang, L. Jiang, Q. H. Wu, et al. "Delay-dependent robust load frequency control for time delay power systems," *IEEE Trans. Power Syst.*, vol. 28, no. 3, pp. 2192–2201, Aug. 2013.

[7] D. J. Teumim. *Industrial network security*. ISA, 2010.

[8] Y. Zhao, W. Yao J. Nan, et al., "Resilient adaptive wide-area damping control to mitigate false data injection attacks," *IEEE Syst. J.*, early access, 2020. Doi: 10.1109/JSYST.2020.3020425.

[9] W. Yao, J. Nan, Y. Zhao, et al. "Resilient wide-area damping control for inter-area oscillations to tolerate deception attacks," *IEEE Trans. Smart Grid*, early access, 2021. Doi: 10.1109/TSG.2021.3068390.

[10] R. Lee, M. Assante, T. Conway. "Analysis of the cyber attack on the Ukrainian power grid," *Electr. Inf. Sharing Anal. Center*, March 2016.

[11] J. P Farwell, R. Rohozinski. "Stuxnet and the future of cyber war," *Survival*, vol. 53, pp. 23–40, Jan. 2011.

[12] A. Sargolzaei, K. Yen, M. N. Abdelghani. "Time-delay switch attack on load frequency control in smart grid," *J. Adv. Commun. Technol.*, vol. 5, pp. 55–64, Nov. 2014.

[13] L. Jiang, W. Yao, Q. H. Wu, et al. "Delay-dependent stability for load frequency control with constant and time-varying delays," *IEEE Trans. Power Syst.*, vol. 27, no. 2, pp. 932–941, May 2012.

[14] L. Jin, C. K.Zhang, Y. He, et al. "Delay-dependent stability analysis of multi-area load frequency control with enhanced accuracy and computation efficiency," *IEEE Trans. Power Syst.*, vol. 34, no. 5, pp. 3687–3696, Sept. 2019.

[15] X. Li, S. Sun. "H_∞ control for networked stochastic non-linear systems with randomly occurring sensor saturations, multiple delays and packet dropouts," *IET Control Theory Appl.*, vol. 11, no. 17, pp. 2954–2963, Nov. 2017.

[16] Y. Shi, B. Yu. "Robust mixed H_2/H_∞ control of networked control systems with random time delays in both forward and backward communication links," *Automatica*, vol. 47, no. 4, pp. 754–760, April 2011.

[17] G. P. Liu, Y. Xia, J. Chen, et al. "Networked predictive control of systems with random network delays in both forward and feedback channels," *IEEE Trans. Ind. Electron.*, vol. 54, no. 3, pp. 1282–1297, April 2007.

[18] Z. H. Pang, W. C. Luo, G. P. Liu and Q. L. Han, "Observer-based incremental predictive control of networked multi-agent systems with random delays and packet dropouts," *IEEE Trans. Circuits Syst. Express Briefs*, vol. 68, no. 1, pp. 426–430, Jan. 2021.

[19] J. Zhang, J. Lam, Y. Xia, "Output feedback delay compensation control for networked control systems with random delays," *Inf. Sci.*, vol. 265, pp. 154–166, May 2014.

[20] W. Tan. "Unified tuning of PID load frequency controller for power systems via IMC," *IEEE Trans. Power Syst.*, vol. 25, no. 1, pp. 341–350, Feb. 2010.

[21] J. Nanda, A. Mangla, S. Suri. "Some new findings on automatic generation control of an interconnected hydrothermal system with conventional controllers," *IEEE Trans. Energy Convers.*, vol. 21, no. 1, pp.187–184, Mar. 2006.

[22] X. C. Shangguan, Y. He, C. K. Zhang, et al. "Control performance standards-oriented event-triggered load frequency control for power systems under limited communication bandwidth," *IEEE Trans. Control Syst. Technol.*, vol. 30, no. 2, pp. 860-868, March 2022.

[23] X. C. Shangguan, Y. He, C. K. Zhang, et al. "Robust load frequency control for power system considering transmission delay and sampling period," *IEEE Trans. Ind. Inf.*, vol. 17, no. 8, pp. 5292-5303, Aug. 2021.

[24] S. Wen, X. Yu, Z. Zeng, J. Wang. "Event-triggering load frequency control for multi-area power systems with communication delays," *IEEE Trans. Ind. Electron.*, vol. 63, no. 2, pp. 1308–1317, Feb. 2016.

[25] C. Peng, J. Zhang, H. Yan. "Adaptive event-triggering H_∞ load frequency control for network-based power systems," *IEEE Trans. Ind. Electron.*, vol. 65, no. 2, pp. 1685–1694, Feb. 2018.

[26] S. Liu, W. Luo, L. Wu. "Co-design of distributed model-based control and event-triggering scheme for load frequency regulation in smart grids," *IEEE Trans. Syst. Man Cybern. Syst.*, vol. 50, no. 9, pp. 3311–3319, Sept. 2020

[27] J. Wang, C. Peng. "Analysis of time delay attacks against power grid stability," *Proc. 2nd Workshop Cyber Phys. Security Resilience Smart Grids*, pp. 67–72, 2017.

[28] A. Sargolzaei, K. K. Yen, M. N. Abdelghani. "Preventing time-delay switch attack on load frequency control in distributed power systems," *IEEE Trans. Smart Grid*, vol. 7, no. 2, pp. 1176–1185, March 2016.

[29] A. Sargolzaei, K. K. Yen, M. N. Abdelghani, et al. "Resilient design of networked control systems under time delay switch attacks, application in smart grid," *IEEE Access*, vol. 5, pp. 15901–15912, July 2017.

[30] H. Zhang, J. Liu, S. Xu. "H-infinity load frequency control of networked power systems via an event-triggered scheme," *IEEE Trans. Ind. Electron.*, vol. 67, no. 8, pp. 7104–7113, Aug. 2020.

[31] K. S. Xiahou, Y. Liu, Q. H. Wu. "Robust load frequency control of power systems against random time-delay attacks," *IEEE Trans. Smart Grid*, vol. 12, no. 1, pp. 909–911, Jan. 2021.

[32] W. Yao, L. Jiang, J. Wen, et al. "Wide-area damping controller for power system interarea oscillations: a networked predictive control approach," *IEEE Trans. Control Syst. Technol.*, vol. 23, no. 1, pp. 27–36, Jan. 2015.

[33] Y. Wu, J. Weng, B. Qiu, et al. "Random delay attack and its applications on load frequency control of power systems," *2019 IEEE Conf. Dependable Secure Computing (DSC). IEEE,* pp. 1-8, 2019.

[34] C. Peng, J. Li, M. Fei. "Resilient event-triggering H_∞ load frequency control for multi-area power systems with energy-limited dos attacks," *IEEE Trans. Power Syst.*, vol. 32, no. 5 pp. 4110-4118, Sep. 2017.